

International Journal on Robotics, Automation and Sciences

Simulation of 500 MHz Electromagnetic Interference Effect on Electrical Equipment with Various RF Grids and Enclosures

Indhika Fauzhan Warsito, Hafild Widyaputera, Eko Supriyanto*, Jaysuman Puspanathan, Mohammad Akmal Abu Taib, and Muhammad Faudzi Mohd Yasir

Abstract— This paper presents the modelling and simulation of a protection system for equipment in the oil and gas industry with various RF grids and enclosures against 500 MHz electromagnetic interference (EMI). COMSOL Multiphysics® Modelling software was used in this study. Electric and magnetic fields distributions were determined by using the Generalized Minimal Residual Method (GMRES) which was integrated into COMSOL Multiphysics® Modelling software. Simulation results indicated that larger RF grid size contributed to the higher electric and magnetic field on equipment. Furthermore, without RF grid, electric and magnetic fields on the equipment were increased significantly (up to 100x). The maximum electric and magnetic fields were found to be near resonance enclosure size (299 mm for 500 MHz frequency source). The results showed that the presence of the RF grid for the EMI protection system was essential.

Keywords—*Electromagnetic Interference, Generalized Minimal Residual.*

I. INTRODUCTION

Nowadays, space is filled up with various kinds of electromagnetic waves, whether they are intentionally or unintentionally [1]. Intentional interference which might be known as intelligent noise is a man-made and intended to be generated to carry certain information. Meanwhile, unintentional interference is naturally generated, which might also be man-made, but is not intended for carrying any sort of information [2]. Overall, Electromagnetic Interference (EMI) can be

caused by electric transmissions, distribution lines, PWM-drive power electronics devices, switching power supplies, and even lightning strikes [3]-[6].

EMI possesses potential harm towards various assets and components. Walkie Talkie, which operates in 500 MHz frequency band, can trigger alarm on a patient vital sign, infant warmer, electrosurgical unit, and even system failure on critical life-saving equipment such as pulse oximeter and incubator [7]. A study by Ouadah and Zergoug analyzed the EMI between power lines and pipelines in oil and gas plants. It turned out that the pipeline was induced with voltage, making it dangerous for the operator to touch them, and the EMI also caused corrosion to the pipelines [7]. Another significant damage is that EMI can cause distortion and noise in the telecommunication system [8]. Other than that, encoders, tachometers, analog signal measurement instrumentations, PLCs and other microprocessor-based components may also be affected by electromagnetic interference.

A mesh common bonding network, or widely known as MESH-CBN, is required to control electromagnetic disturbances at a boundary of the electromagnetic zone. The mesh behaves as a shield that attenuates radiated EM phenomena as well as operating as an RF Reference Plane for equipment within the EM Zone.

Individual mesh elements in the boundary should have their diagonals much less than $50/f_{max}$, as shown in Figure. 1 [9]. Mesh with element diagonals

*Corresponding author. Email : eko@utm.my

ORCID: 0000-0002-6766-793X

Indhika Fauzhan Warsito is with E-Life Solutions PLT, Johor Bahru 81310, Malaysia and School of Biomedical Engineering and Health Sciences, Faculty of Engineering, Universiti Teknologi Malaysia (e-mail: dhika@elife-solutions.com)

Hafild Widyaputera is with E-Life Solutions PLT, Johor Bahru, 8310, Malaysia (e-mail: hafild.dimas@gmail.com).

Eko Supriyanto is with Advanced Diagnostics and Progressive Human Care Research Group, IJN-UTM Cardiovascular Engineering Center, Institute of Human Centered Engineering, School of Biomedical Engineering and Health Sciences, Faculty of Engineering, Universiti Teknologi Malaysia 81310 Johor Bahru, Malaysia (email: eko@utm.my)

Jaysuman Puspanathan is with Universiti Teknologi Malaysia, Johor Bahru 81310, Malaysia (email: jaysuman@utm.my)

Mohammad Akmal Abu Taib and Muhammad Faudzi Mohd Yasir are with Petrolia Nasional Berhad, Malaysia

of $150/f$ or larger provides no EMC benefit and could resonate and make their EM Zone's characteristic worse than having no EM zoning at all.

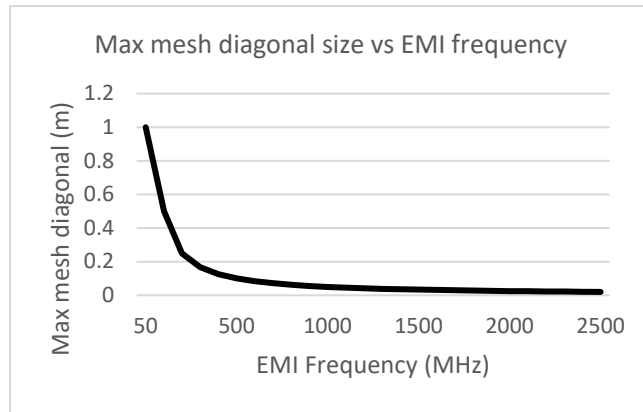


FIGURE 1. Recommended maximum mesh diagonal ($\lambda/20$) respective to EM frequency.

Due to their sensitivity over external electromagnetic radiation, electronic systems require the corresponding shielding. With a careful connection to the surrounding ground, a Faraday cage can be created, with an attenuation value up to 60 decibels (1:1.000.000) [10]. All conductive materials are suitable for performing these tasks. However, the shielding effect increases together with the specific conductivity of the metal.

For typical commercial and industrial computer and telecommunication rooms, the best practice is to create a System Reference Potential Plane (SRPP) for each system block from a local bonding mat. Wire with 6mm diameter or larger and 25 x 3mm copper strip is often used to create bonding mat meshes. The mesh size should be related to the desired frequencies which are controllable and should not more than $1/20$ of the shortest wavelength [11].

Smaller mesh size provides better EMI frequencies attenuation control. Additionally, a Continuous Bonding Conductor (BRC) which surrounds the bonding mat, should be bonded to all conductors on the mat. The size and shape of the BRC depend on the perimeter of the building. A smaller system block might take up a significant part of the whole floor. Ideally, both vertical and horizontal CBN meshes should not be more than 3-meter square in size [12].

Furthermore, resonance frequency corresponds to the physical dimension of the cavity (i.e. enclosure). The danger of cavity resonance is a large field that can be generated at this frequency due to the multiplication or amplification effect if a noise source has a frequency component which corresponds to a resonant point [10]. Resonance frequency formula due to a cavity in block shape is

$$(f)_{mnp} = \frac{1}{2\sqrt{\epsilon\mu}} \sqrt{\left(\frac{m}{a}\right)^2 + \left(\frac{n}{b}\right)^2 + \left(\frac{p}{c}\right)^2} \quad (1)$$

where ϵ is material permittivity, μ is material permeability, a, b , and c are shape parameters, m, n , and p are integer constants [12].

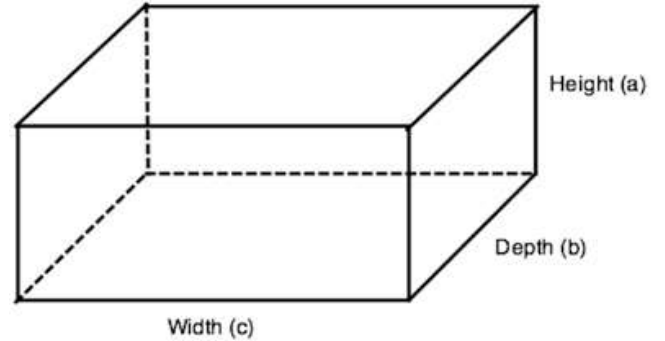


FIGURE 2. Block parameters for cavity frequency resonance.

Furthermore, as derived from equation (1), we can determine the enclosure side size (i.e. enclosure shape is cube) where resonance happens on the specific frequency with the following formula

$$(d)_{mnp} = \frac{1}{2f\sqrt{\epsilon\mu}} \sqrt{(m)^2 + (n)^2 + (p)^2} \quad (2)$$

where d is enclosure side size (i.e cube).

In this study, our objective is to identify electric and magnetic fields effects at 500 MHz frequency RF source band with different RF ground sizes and enclosure sizes.

II. MODELLING AND SIMULATION PARAMETERS

In this paper, the modelling and simulations were carried out by using COMSOL software (ver. 5.3). To simplify the modelling, the electric equipment was modelled in cubic shape. Meanwhile, the enclosure was shaped similarly, surrounding the equipment model. The equipment was put inside the enclosure. In this simulation, a log-periodic antenna was used to generate electromagnetic (EM) interference on 500 MHz frequency (figure 3). In this study, Electromagnetic Waves, Frequency Domain Interface, and Far Field Domain were selected to enable primary power transfer via radiation.

A. Simulation variations

In this study, there were two different enclosure models. Enclosure type A covered the entire equipment with no gap between the enclosure's inner surface and equipment. On the other hand, enclosure type B was a hollow cube which provide a gap between the enclosure's inner surface and the equipment.

With enclosure type A configuration, the significance of RF grid reference was inspected by simulating various RF grid size, including a configuration where there was no RF grid at all. Figure

4 shows the modelling with RF grid reference, while Figure 5 shows the modelling with no RF grid reference.

Other than that, variations of grid size were also simulated to determine the optimal mesh size of the grid. According to the explanation in the previous section, the individual mesh diagonal should not surpass $50/f_{\max}$. Hence, the maximum mesh size for protection against 500 MHz EMI is 0.07m. There were five different grid configurations under the perfect enclosure condition. One of the configurations had no MESH-CBN at all, while the other two had mesh size more than the maximum limit. Meanwhile, the other two had mesh size less than 0.07m. Overall, the mesh size variations were 0.25m, 0.13m, 0.063m, 0.025m, and no grid at all. In the other hand, under real enclosure, there were three variations of mesh size: 0.25m, 0.125m, and 0.0125m. The first two variations surpassed the maximum mesh size limit, while the last one did not. Later, the difference between mesh size more and less than the limit was also observed.

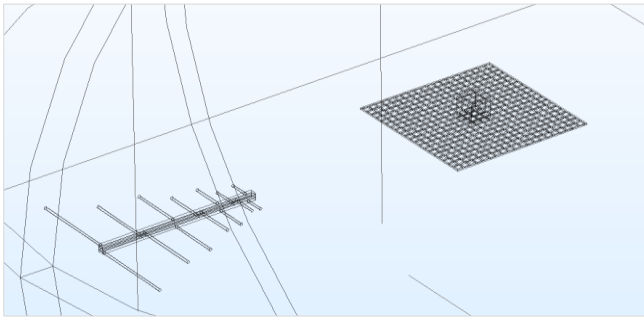


FIGURE 3. Simulation configuration.

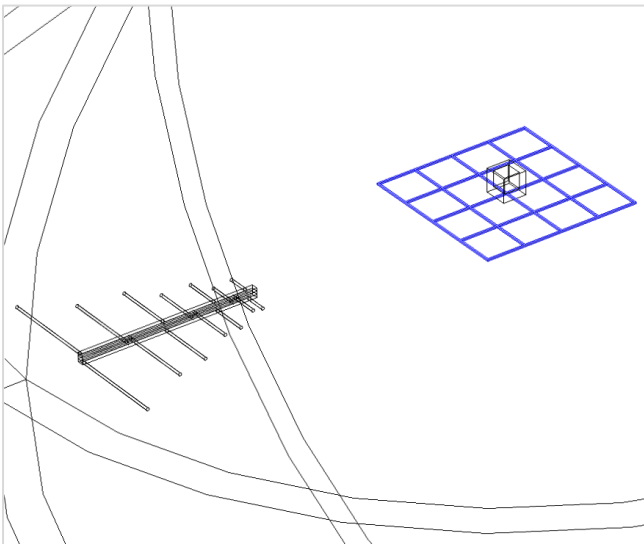


FIGURE 4. A simulation model with RF grid reference.

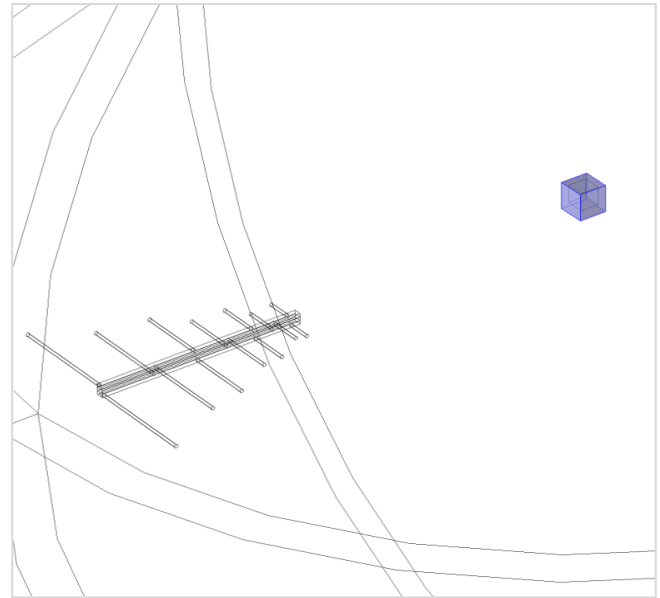


FIGURE 5. Simulation model without RF grid reference.

B. Simulation Parameters

In the simulation, aluminum with electrical conductivity, σ of 3.77×10^7 S/m was used for the enclosure; iron with σ of 1.12×10^7 S/m was used for the equipment; copper with σ of 5.99×10^7 S/m was used for the grid and the remaining empty space was filled up with air ($\sigma=0$ S/m).

In this study, the electromagnetic interference's frequency was set to 500 MHz. This frequency is considered to be Ultra High Frequency (UHF). Radio communication such as walkie-talkie operates around this range of frequency.

III. RESULTS AND ANALYSIS

A. Effect of RF grid variation

Overall, there were five variations of grid mesh size under perfect enclosure (type A) condition. TABLE 1. and Table TABLE 2. show the average electric and magnetic field level on the surface of the enclosure and the equipment. Meanwhile, from Figure 6 to Figure 9 showed that the trend of the electromagnetic field on various mesh sizes.

As can be seen in Table 1 and Table 2, the presence of an enclosure and the CBN grounding mat resulted in significant electric and magnetic field drop. When no grounding grid (*no mesh*) was being used, the electric field on equipment reached as high as 100 times higher than using 0.025mm mesh. Meanwhile, the magnetic field was about 50 times higher. Generally, the trend shows that the electric and magnetic field increased when the mesh size was bigger (both on the equipment and the enclosure). In the simulation with smaller mesh size, the total conductor length was obviously higher. Hence, the total impedance of the grounding grid was smaller. A grounding grid with less impedance would allow the induced EMI to disperse

faster. Consequently, the EMI protection provided better attenuation. Hence, in the condition with no RF grid at all (meaning no conductor was being used), the results showed the highest electric and magnetic fields among all simulations.

TABLE 1. Electric Field on Mesh Size Variations under Enclosure type A.

Mesh size (m)	Electric Field (V/m)	
	<i>Enclosure</i>	<i>Equipment</i>
0.025	0.09	1.03E-11
0.063	0.17	1.20E-11
0.125	0.25	1.70E-11
0.25	0.27	1.61E-11
No mesh	0.70	1.0588E-09

TABLE 2. Magnetic Field on Mesh Size Variations under Enclosure type A.

Mesh size (m)	Magnetic Field (A/m)	
	<i>Enclosure</i>	<i>Equipment</i>
0.025	1.37E-03	7.92E-12
0.063	1.42E-03	9.62E-12
0.125	2.03E-03	1.45E-11
0.25	3.13E-03	1.36E-11
No mesh	3.62E-03	4.86E-10

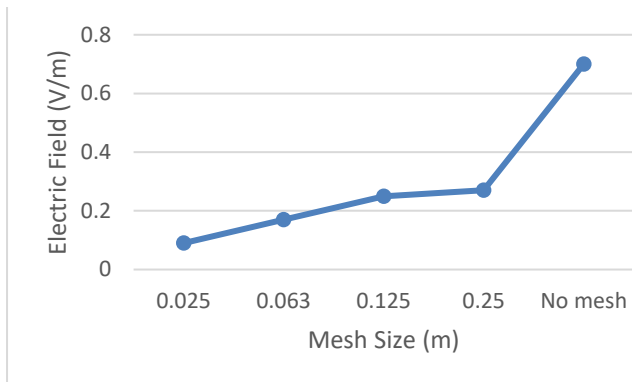


FIGURE 6. Electric field on enclosure, mesh size variations under enclosure type A.

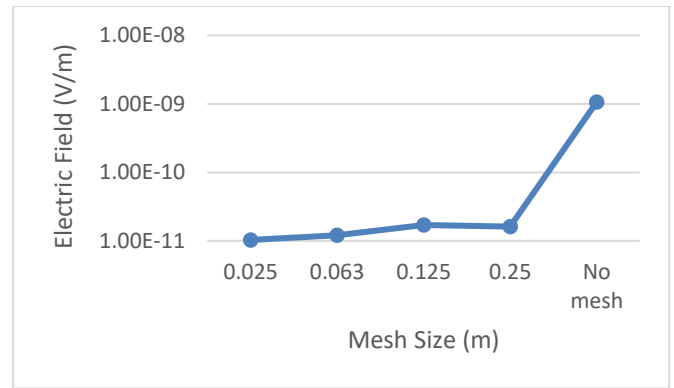


FIGURE 7. Electric field on equipment, mesh size variations under enclosure type A.

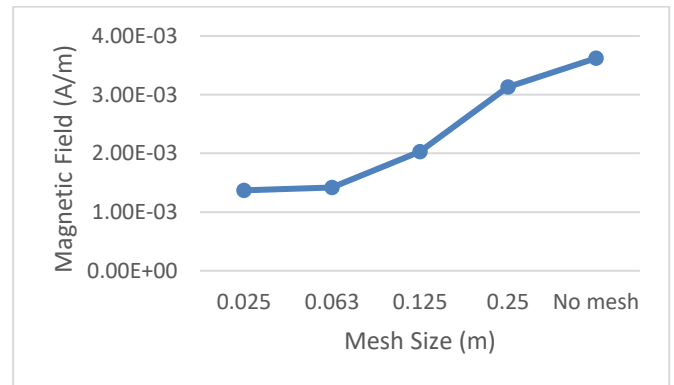


FIGURE 8. Magnetic field on enclosure, mesh size variations under enclosure type A.

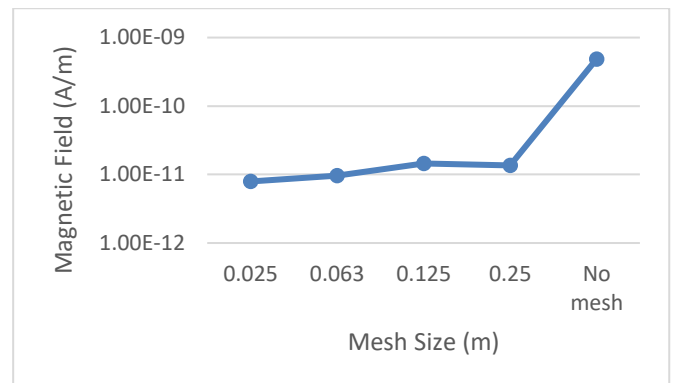


FIGURE 9. Magnetic field on equipment, mesh size variations under enclosure type A.

In Figure 8, it was observed that the grid with mesh size of 0.063m provided significantly better magnetic protection than the bigger mesh sizes. As explained in section 2, the MESH-CBN provided optimum attenuation for mesh diagonal less than $50/f_{max}$. Furthermore, in section 3, the maximum mesh size limit was obtained as 0.07m. Hence, only the 0.063 and 0.025m mesh size complied with this rule. Moreover, the 0.025m mesh size produced a similar magnetic field protection level compared to 0.063m mesh size. Therefore, decreasing the mesh size from 0.063 to 0.025m was considered not efficient.

Furthermore, from Figure 10 to Figure 13 illustrated the electric and magnetic fields distributions throughout the surrounding of the equipment. The various colorizations depicted the different levels of

electric field and magnetic fields. Each of the levels is described on the chart next to the respective picture.

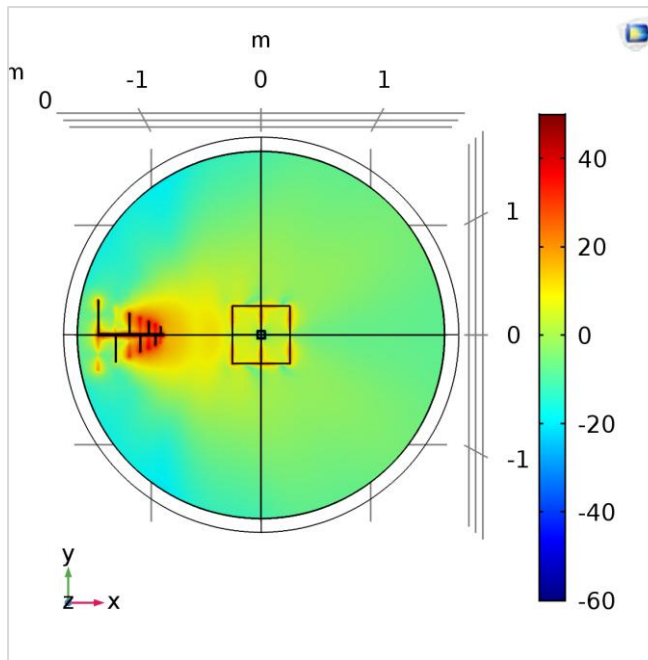


FIGURE 10. Electric field on 0.25m mesh size under enclosure type A.

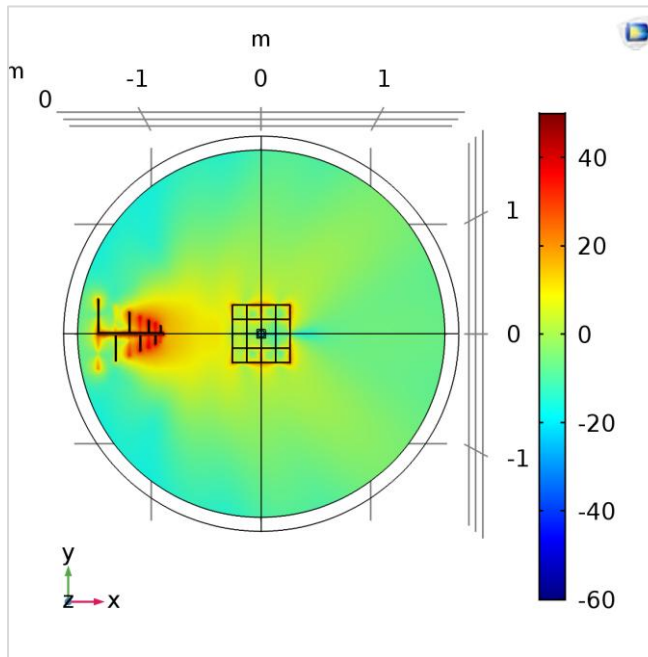


FIGURE 11. Electric field on 0.125m mesh size under enclosure type A.

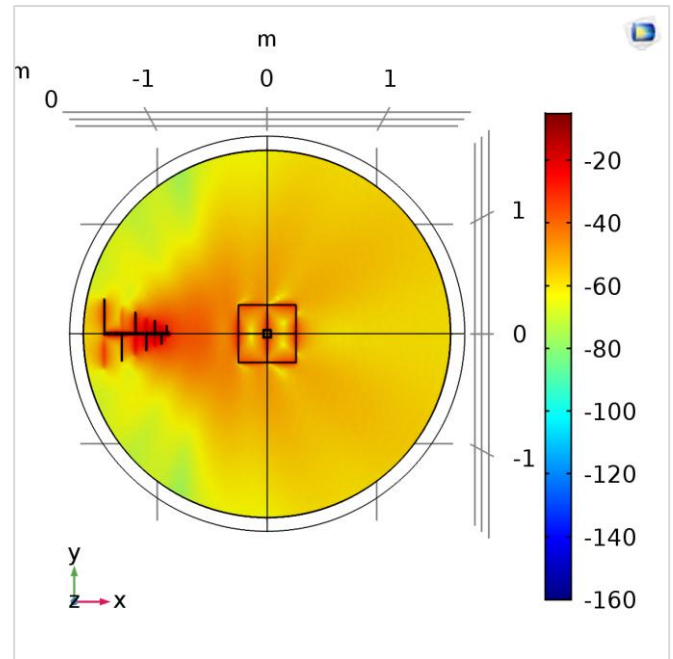


FIGURE 12. Magnetic field on 0.25m mesh size under enclosure type A.

From the figures, it was observed that the electric and magnetic fields decreased as the observation point grew apart from the antenna. Furthermore, from Figure 10 to Figure 13, there were no significant differences in the EMI level throughout the surrounding area. As explained in [9], the EMI protection did not produce attenuation for the space outside the protection zone.

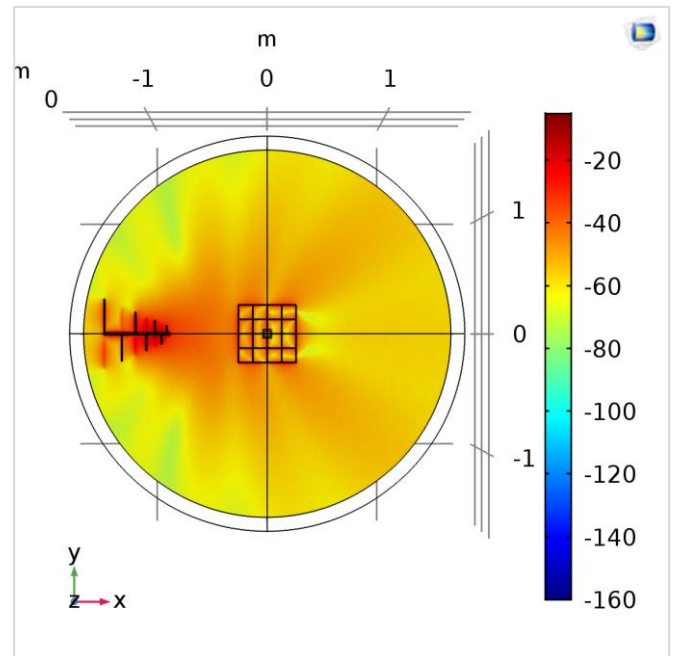


FIGURE 13. Magnetic field on 0.125m mesh size under enclosure type A.

B. Effect of enclosure size variation

In this study, ten variations of the enclosure size were simulated (figure 2) by using the enclosure type B configuration. Table 3 and Table 4 show the electric

and magnetic field which were produced on the enclosure and on the equipment. Meanwhile, from Figure 14 to Figure 17 showed the trend of the electromagnetic field on various enclosure side sizes.

TABLE 3. Electric Field on enclosure side size variations with enclosure type B.

Enclosure Side Size (mm)	Electric Field (V/m)	
	Enclosure	Equipment
50	0.2160	0.0188
75	0.2933	0.0235
100	0.3958	0.0215
125	0.5011	0.0355
150	0.4790	0.1212
175	0.3988	0.2344
200	0.7699	0.3340
250	1.2186	0.4694
275	0.7517	0.4152
300	0.6447	0.3328

TABLE 4. Magnetic Field on Mesh Size Variations under Enclosure type B.

Enclosure Side Size (mm)	Magnetic Field (mA/m)	
	Enclosure	Equipment
50	3.0322	0.3015
75	2.2018	0.1371
100	1.9967	0.1188
125	2.2722	0.3439
150	2.8649	0.7223
175	2.7248	1.0000
200	2.8500	1.1407
250	3.8977	1.3754
275	4.4697	1.0104
300	4.6502	0.8098

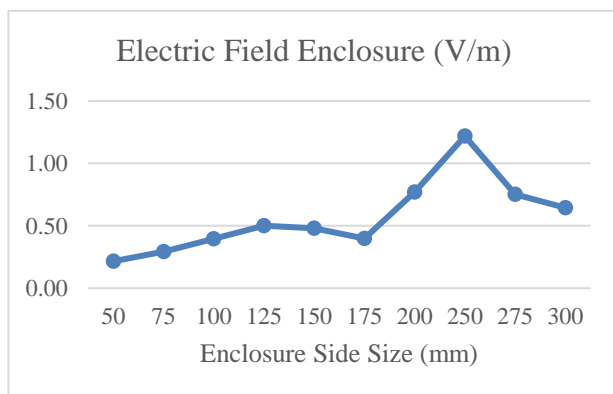


FIGURE 14. Electric field on enclosure surface, variation of enclosure side size.

In formula (2), it was found that resonance due to cavity shape at 500 MHz happened when enclosure size was 299 mm ($m=1, n=0, p=0$). It was observed that from Figure 14 to Figure 17, electric and magnetic fields on enclosure and equipment were near maximum value when enclosure side size was 299 mm. Similar result was also obtained when the enclosure side size was near 250 mm.

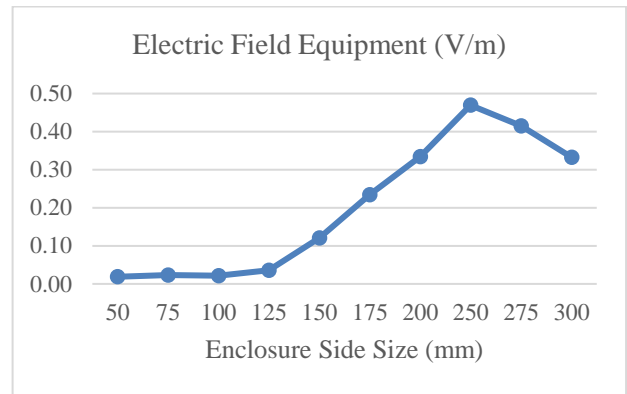


FIGURE 15. Electric field on equipment surface, variation of enclosure side size.

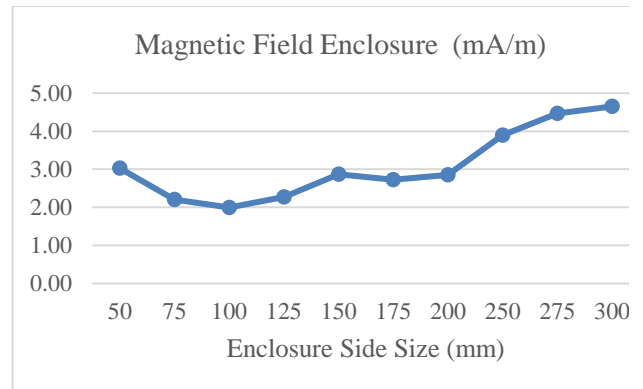


FIGURE 16. Magnetic field on enclosure surface, variation of enclosure side size.

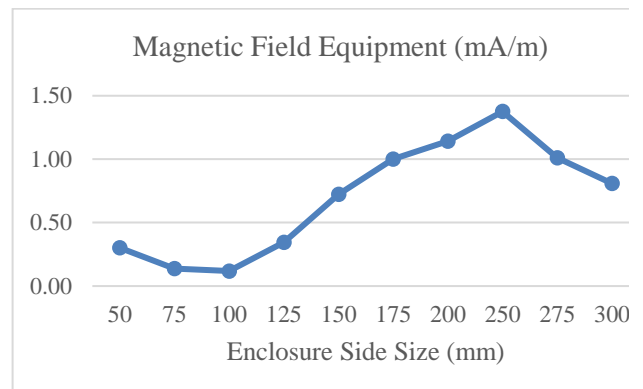


FIGURE 17. Magnetic field on equipment surface, variation of enclosure side size.

IV. CONCLUSION

The equipment, enclosure, grid, and the antenna had been modelled in order to study the effects of

electromagnetic interference on various EMI protection models. The simulation results showed that the electric and magnetic fields increased when the mesh size increased. Usage of grounding grid or RF references was important as it provided significant improvement to reduce electric and magnetic fields interference on the equipment and its enclosure. Furthermore, based on simulation results, it could be seen that the electric and magnetic field at 500 MHz reached their maximum value when the enclosure side size was 299 mm.

ACKNOWLEDGMENT

We thank the anonymous reviewers for the careful review of our manuscript.

FUNDING STATEMENT

This work was supported in part by the Ministry of Higher Education Malaysia, Universiti Teknologi Malaysia under Grant GUP 16H82, E-Life Solutions PLT, and Petroliaam Nasional Berhad, Malaysia.

AUTHOR CONTRIBUTIONS

Indhika Fauzhan Warsito: Conceptualization, Methodology, Validation, Writing – Original Draft Preparation;

Hafild Widyaputera: Literature Review;

Eko Supriyanto: Project Administration, Supervision, Writing – Review & Editing;

Jaysuman Pusppanathan: Data Curation, Validation;

Mohammad Akmal Abu Taib: Data Curation, Simulation;

Muhammad Faudzi Mohd Yasir: Validation, Writing – Review & Editing.

CONFLICT OF INTERESTS

No conflict of interests was disclosed.

ETHICS STATEMENTS

Our research work follows The Committee of Publication Ethics (COPE) guideline. <https://publicationethics.org>.

REFERENCES

- [1] X. Li, X. Hao, L. Wang, Y. Zeng and H. Han, "Research on in-band electromagnetic interference effect of communication system," in *2016 IEEE MTT-S International Microwave Workshop Series on Advanced Materials and Processes for RF and THz Applications (IMWS-AMP)*, pp. 1-4, 2016. DOI: <https://doi.org/10.1109/IMWS-AMP.2016.7588452>
- [2] D. Middleton, "Statistical-physical models of electromagnetic interference," *IEEE Transactions on Electromagnetic Compatibility*, vol. 3, pp. 106-127, 1977. DOI: <https://doi.org/10.1109/TEMC.1977.303527>
- [3] F. Lin and D. Y. Chen, "Reduction of power supply EMI emission by switching frequency modulation," *IEEE Transactions on Power Electronics*, vol. 9, no. 1, pp. 132-137, 1994. DOI: <https://doi.org/10.1109/PESC.1993.472080>
- [4] H. Akagi and T. Shimizu, "Attenuation of conducted EMI emissions from an inverter-driven motor," *IEEE Transactions on Power Electronics*, vol. 23, no. 1, pp. 282-290, 2008. DOI: <https://doi.org/10.1109/TPEL.2007.911878>
- [5] M. H. Shwehdi, "A Practical Study of an electromagnetic interference (EMI) problem from Saudi Arabia," in *2004 Large Engineering Systems Conference on Power Engineering (IEEE Cat. No.04EX819)*, pp. 162-169, 2004. DOI: <https://doi.org/10.1109/LESCPE.2004.1356293>
- [6] G. Xuehai and H. Jinliang, "Electromagnetic Interference on Secondary Systems of Substation Caused by Incoming Lightning Stroke," in *2007 IEEE International Symposium on Electromagnetic Compatibility*, pp. 212-216, 2007. DOI: <https://doi.org/10.1109/ELMAGC.2007.4413468>
- [7] D. B. Stroud, Y. Huang, L. Hansen and R. McKenzie, "Walkie talkies cause more electromagnetic interference to medical equipment than mobile phones," *Australasian Physics & Engineering Sciences in Medicine*, vol. 29, no. 4, pp. 315, 2006. DOI: <https://doi.org/10.1007/BF03178397>
- [8] C. Munteanu, V. Topa, G. Mates, M. Purcar, A. Racasan and I. T. Pop, "Analysis of the electromagnetic interferences between overhead power lines and buried pipelines," in *IEEE International Symposium on Electromagnetic Compatibility-EMC EUROPE*, pp. 1-6, 2012. DOI: <https://doi.org/10.1109/EMCEurope.2012.6396746>
- [9] A. Ghose and G. Deb, "Electromagnetic interference impact on communication tests," *Proceedings of the International Conference on Electromagnetic Interference and Compatibility '99 (IEEE Cat. No. 99TH 8487)*, pp. 213-216, 1997. DOI: <https://doi.org/10.1109/ICEMIC.1997.669800>
- [10] Z. Shahriari, R. Leewe, M. Moallem and K. Fong, "Automated Tuning of Resonance Frequency in an RF Cavity Resonator," in *IEEE/ASME Transactions on Mechatronics*, vol. 23, no. 1, pp. 311-320, 2018. DOI: <https://doi.org/10.1109/TMECH.2017.2772183>
- [11] R. L. Kobus, R. L. Skaggs, M. Bobrow, S. A. Kliment, J. Thomas and T. M. Payette, *Building type basics for healthcare facilities*, vol. 13, John Wiley & Sons, 2008.
- [12] S. Theepak, V. S. Namburi, B. Devadas and R. Selvapriya, "Mitigation of resonance in RF high power amplifier enclosure," in *2017 IEEE Topical Conference on RF/Microwave Power Amplifiers for Radio and Wireless Applications (PAWR)*, pp. 104-107, 2017. DOI: <https://doi.org/10.1109/PAWR.2017.7875585>